Contents lists available at: http://qu.edu.iq

Al-Qadisiyah Journal for Engineering Sciences

Journal homepage: https://qjes.qu.edu.iq

Research Paper

Influence of joule heating and exponential heat source on the cassonfluid flow through a thermally graded permeable medium

***G. Raghavendra Ganesh* [1], *Shaik Jaffrullah* [2], *Wuriti Sridhar* [3], *Khaled Al-Farhany* [4,5], *Mohamed F. Al-Dawody* [4], *and Mujtaba A. Flayyih* [6]**

[1] *Department of Mathematics, PVP Siddhartha Institute of Technology, Kanuru, Vijayawada, A.P., India.*
[2] *Department of Mathematics, Amrita Sai Institute of Science and Technology, Paritala, NTR Dist, A.P., India.*
[3] *Department of Mathematics, Koneru Lakshmaiah Education Foundation, Vaddeswaram, Guntur, India.*
[4] *Department of Mechanical Engineering, College of Engineering, University of Al-Qadisiyah, Al-Qadisiyah, Iraq.*
[5] *College of Engineering, University of Warith Al-Anbiyaa, Karbala, Iraq.*
[6] *Biomedical Engineering Department, College of Engineering and Technologies, Al-Mustaqbal University, Hillah, Iraq.*

ARTICLE INFO

Article history:
Received 17 April 2024
Received in revised form 22 February 2025
Accepted 15 August 2025

keyword:
Casson fluid
Porous media
Thermal stratification
MHD
Joule heating
Exponential heat source
Chemical reaction

ABSTRACT

The work aims to investigate the MHD Casson fluid flow over an exponentially long sheet via a thermally stratified permeable medium. All facets of chemical processes, Joule heating, and exponential heat sources are covered in this subject. By using the appropriate similarity conversions, the leading partial differential equations (PDEs) of the model are transformed into a set of nonlinear ordinary differential equations (ODEs). The description of the previous technique was made simpler by applying the Keller Box methodology. The results reveal that when the viscosity factor is increased, the velocity profile improves, but when the thermal profile improves, the opposite trending impact is evident. The temperature profile exhibits the opposite tendency, despite a decline in the number of observations of the Casson fluid constraint. Joule heating parameters allow for more precise measurements of the heat source's properties by raising the temperature. The concentration graph shows a reduction as the number of observations for the chemical reaction parameter increases. The validity of the problem is investigated by computing the Nusselt number for cumulative Prandtl number observations and comparing the results with the literature.

1. Introduction

According to Shenoy [1], non-Newtonian fluid streams that transfer mass and heat are used in many different industries, including food processing, polymer processing, oil and gas extraction, biomedical engineering, and oil and gas extraction. When Chamka and Humoud [2] used the finite difference technique to study the typical characteristics of a Power law fluid over an upright plate, they discovered that the amount of heat transfer increased with an increase in the buoyancy ratio factor. Research conducted by Kairi and Murthy [3] on non-Newtonian fluid flow on a vertical cone demonstrates that when the viscous dissipation parameter increases, the Nusselt number decreases. According to Gorla et al. [4], the study of non-Newtonian fluids has several practical applications in a wide range of industries and may be applied to a wide variety of flow situations. The food processing business and the polymer industry are two of these domains. According to studies by Sinha and Shit [5] on the impact of the velocity slip parameter on blood flow characteristics, the heat conductivity parameter determines the temperature of blood. When Eldabe et al. [6] studied a Casson fluid model on a moving wedge using the differential transform method, they found that the velocity distribution decreased as the strength of the magnetic field increased. Singh and Yadav [7] examined the properties of non-Newtonian fluid heat transfer and discovered that the fluid velocity and the coefficient of heat transmission increased with the permeability limit. This was one of the findings from each of their studies. MHD is widely used in a variety of fields due to its ability to apply magnetic fields to regulate and alter fluid flow. The Casson fluid rheological model finds applications in the fields of drilling fluids and biomedical engineering. It offers a simple way to refer to the fluid flow performance affected by yield stress. Vajravelu et al. [8] investigated the Casson fluid model on a vertically expanding sheet and discovered that when the Casson parameter is increased, the velocity boundary layer's breadth narrows. As the suction constraint temperature dropped, Attia and Ahmed [9] investigated the heat relocation properties of the Casson fluid stream between parallel plates. Researchers Shehzad et al.[10] looked studied the mass relocation properties of Casson fluid flows over an expanding sheet as well as the magnetic parameter of the concentration boundary layer. Thickness rises. In their investigation [11], Gireesha et al. looked at the Casson fluid flow over a long absorbent sheet. Apply Fehlberg Runge-Kutta technique. For more accurate measurements of the Casson parameter and the magnetic factor, the momentum barrier layer must be made thinner. As the Casson constraint observations increased, Animasaun's work [12] indicated a diminishing trend in the temperature profile of the Casson fluid flow over a perpendicular permeable plate with higher-order chemical processes. Hussanan et al. developed a flow system using Casson fluid on a nonlinearly elongating sheet where fluid temperature decreases with increasing Prandtl numbers[13]. Ibrahim et al. investigated the Casson fluid flow over a sheet with exponential permeability [14].

*Corresponding Author.
E-mail address: khaled.alfarhany@yahoo.com ; Tel: (+964) 783-076 3523 (Khaled Al-Farhany)

https://doi.org/10.30772/qjes.2025.163822.1687

Nomenclature

b,c,d	Constants	T_o	Reference temperature
C	Concentration of fluid	T_w	Temperature at surface
C_o	Reference concentration	T_∞	Ambient temperature
C_w	Concentration of the surface	u,v	Velocity components
C_∞	Ambient concentration temperature	*Greek Symbols*	
D_b	Brownian diffusion	ν	Kinematic viscosity
g	Gravity constant	σ	Electrical conductivity
J	Joule heating parameter	β	Casson parameter
k	Permeability of the porous medium	q_r	Radiative heat flux
K_c	Chemical reaction parameter	ε	Thermal conductivity parameter
M	Magnetic parameter	ρ	Density of fluid
N	Stretching sheet parameter	c_p	Specific heat of the fluid
Pr	Prandtl number	k^*	Thermal conductivity
Q_o	Heat source	β^+	Thermal expansion coefficient
q_1	Heat source index	ζ	Plastic dynamic viscosity parameter
Sc	Schmidt number	γ	Conjugate Newtonian parameter
T	Temperature of the fluid		

Utilizing the HAM radio equipment. They discovered that compared to Newtonian fluid, the rate of heat transmission in Casson fluid is faster. In a subsequent work, Ganesh and Sridhar examined the behavior of Casson nanofluid flow on a non-linear expanding surface [15]. They found that concentration profiles get more pronounced with increasing Casson parameter. Sridhar et al. [16] investigated the Casson fluid stream across a porous stretched electromagnetic plate. Temperature augmentation was observed in the radiation parameter condition. Printed circuit boards, resistive heating components, electric welding, and medicinal applications are among the uses of Joule heating in electrical appliances. Khaled et al. [17] experimentally investigated heat transfer in a cavity loaded with (50% CuO-50% Al2O3)/Water with a hybrid nanofluid connected to a vertically heated wall partially integrated with PCM methodology. Ghurban et al. [18] numerically investigated the effects of a fin on mixed convection heat transfer in a vented square cavity. Kamran et al.'s study on joule-heated nanofluid flow was conducted [19]. We are tracking the Eckert number bit by bit. Ghiasi and Saleh [20] pointed out that magnetic entropy generation is a helpful method for figuring out the irreversibility of the Joule heating process in their study of Casson fluid flow. According to Goud et al.'s study [21] of the Casson nanofluid stream on an inclined porous stretched sheet subjected to joule heating, skin friction decreases when the joule heating parameter is raised. Jaffrullah et al.'s study [22] examined the Casson fluid flow in a Darcy-Forchheimer absorbent channel with Joule heating present. They discovered that the temperature rose in tandem with the joule heating parameter. Research by Makinde et al. [23] showed that species concentration increases with n-order chemical processes. The study looked at the flow of a Boussinesq liquid under an n-order reaction on a plate with vertical pores. Using an expanded sheet, Shawky [24] looked into the Casson liquid's direction. As the Schmidt number rises, the liquid concentration falls. Slip factors, according to Mabood et al. [25], reduce the velocities of these two kinds of transfers. They also looked at the mass and heat relocation aspects of Casson fluid flow. Al-Naib et al [26] investigated the heat transfer characteristics of Al2O3-water nanofluid in a coiled agitated vessel across varied operating conditions. Ganesh and Sridhar [27] looked into the effects of chemical reactions on the Casson fluid stream across a movable plate. They found that concentration profiles diminish when a chemical process is intensified. Mahesh et al. [28] discovered that the rate of heat relocation increases with increasing observations of the volume fraction parameter when they examined the Marangoni outer layer course of a Casson fluid using the incomplete Gamma function technique. Heat exchangers, cooling systems, chemical and biological processes, environmental remediation, oil and gas reservoirs, and more are applications for stratified porous media. Nuclear engineering, healthcare applications, and material processing are among the fields in which exponential heat sources find application. Yusuf et al. [29] conducted an entropy exploration investigation of a Casson fluid stream moving across a curved stretching sheet. They found that decreasing the heat source increased the species' molecular reaction. According to Pattnaik et al.'s research [30], exponential heat creation is the main factor in the thermally based heat generating method. Waqas et al. looked into the bio-convectional flow of burger fluid. [31] observed that when the exponential heat generation factor crosses a specific threshold, temperature augmentation becomes apparent. Kumar et al. [32] examined a Cu-polyvinyl alcohol-based Jeffrey fluid stream on a non-linear vertical extending sheet. The Nusselt number decreases as the exponential heat source characteristics increase in value. Dagan [33] investigated the flow and heat transfer characteristics of various porous formation types. According to Malik et al.'s research [34], the temperature of the Casson fluid flow on the slanted sheet with viscid dissipation decreases as the stratification parameter increases. According to research on the Casson fluid course through thermally stratified permeable media over an exponentially elongated sheet with exponential heat generation, Agrawal et al. [35] found that when stratification is absent, an increase in the Casson factor lowers the velocity profile, but when stratification is present, a reverse trend is observed. In the present work, a two-dimensional Casson fluid flow over a thermally stratified absorbent material is investigated, considering both Joule heating and chemical reaction.

2. Problem Formulation

An analysis is conducted on a 2-D flow of a Casson fluid via a surface that is exponentially stretched in the presence of stratified porous media. The magnetic field is applied in conjunction with the effects of an exponential heat source, Joule heating, and chemical reaction as shown in Fig. 1.

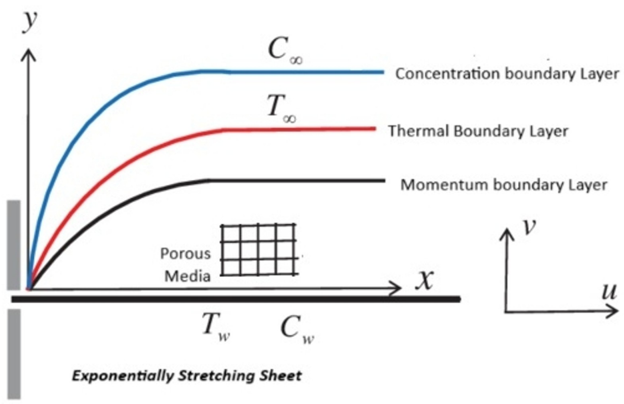

Figure 1. Flow model of the problem.

Under these conjectures, the equations that control the problem are considered as Eqs. 1, 2, 3 and 4:

$$\frac{\partial u}{\partial x}+\frac{\partial v}{\partial y}=0 \tag{1}$$

$$u\frac{\partial u}{\partial x}+v\frac{\partial u}{\partial y}=\nu\frac{\partial^2 u}{\partial y^2}-\frac{\nu u}{k}-\sigma\frac{B^2(x)}{\rho}u+gB^+(T-T_\infty) \tag{2}$$

$$u\frac{\partial T}{\partial x}+v\frac{\partial T}{\partial y}=\frac{k^*}{\rho c_p}\frac{\partial^2 T}{\partial y^2}-\frac{1}{\rho c_p}\frac{\partial q_r}{\partial y}+ +\sigma\frac{B^2(x)}{\rho c_p}u^2+\frac{Q_o}{\rho c_p}(T_w-T_\infty)e^{-\eta y\sqrt{\frac{U_o}{2\nu L}}}\,e^{\frac{x}{2L}} \tag{3}$$

$$u\frac{\partial C}{\partial x}+v\frac{\partial C}{\partial y}=D_B\frac{\partial^2 C}{\partial y^2}-K_1(C-C_\infty) \tag{4}$$

Where $\nu=\frac{\mu_b}{\rho}\left(1+\frac{1}{\beta}\right)$ is the kinematic viscosity of Casson fluid and $B(x)=B_o e^{\frac{x}{2L}}$ is the strength of the magnetic field. Subject to the following boundary conditions, Eq. 5.

$$\left.\begin{aligned} u = u_w(x) &= U_o\, e^{\frac{x}{2L}} \\ v_w(x) &= v_o\, e^{\frac{x}{2L}} \\ T_w(x) &= T_o + b\, e^{\frac{x}{2L}} \\ T_\infty(x) &= T_o + c\, e^{\frac{x}{2L}} \\ C_w(x) &= C_o + d\, e^{\frac{x}{2L}} \end{aligned}\right\} \tag{5}$$

Using similarity transformations, Eq. 6.

$$\left.\begin{aligned} \psi &= \sqrt{2vLU_o} f(\eta)\, e^{\frac{x}{2L}} \\ \eta &= y\sqrt{\frac{U_o}{2vL}}\, e^{\frac{x}{2L}} \\ \theta(\eta)(T_w - T_\infty) &= T - T_\infty \\ \phi(\eta)(C_w - C_o) &= C - C_\infty \end{aligned}\right\} \tag{6}$$

The Eqs. 2 - 4 are converted to Eqs. 7 - 9.

$$\left(1+\frac{1}{\beta}\right)(1+\zeta-\theta\zeta-\zeta S_t)f''' - \zeta\left(\frac{1}{\beta}+1\right)\theta' f'' - - Mf' + G_{rm}\theta\zeta - 2f'^2 = 0 \tag{7}$$

$$\left(1+\varepsilon\theta+\frac{4}{3N}\right)\theta'' + \varepsilon\theta'^2 - PrS_t f' + Pr\theta f' + Prq_1 e^{-n\eta} + + PrJf'^2 + Prf\theta' = 0 \tag{8}$$

$$\phi'' - Sc\gamma\phi + Scf\phi' = 0 \tag{9}$$

The numerical methodology, Eq. 10.

$$\left.\begin{aligned} \frac{df}{d\eta} = p \;;\quad \frac{dp}{d\eta} = q \\ \frac{dg}{d\eta} = t \;;\quad \frac{ds}{d\eta} = n \end{aligned}\right\} \tag{10}$$

Where $g = \theta$, $s = \phi$, then the Eqs. 7 - 9 are altered to Eqs. 11 - 13.

$$(1+\zeta-\theta\zeta-\zeta S_t)q' - \zeta tq - 2\left(\frac{\beta}{\beta+1}\right)p^2 - \left(\frac{\beta}{\beta+1}\right)Mp + + \left(\frac{\beta}{\beta+1}\right)G_{rm}g\zeta = 0 \tag{11}$$

$$\left(1+\varepsilon\theta+\frac{4}{3N}\right)t' + \varepsilon t^2 + Prft - PrS_t p - Prgp + + Prq_t e^{-n\eta} + PrJp^2 = 0 \tag{12}$$

$$n' - Sc\gamma s + Scfn = 0 \tag{13}$$

As well as, the boundary conditions are transformed to Eq. 14.

$$\left.\begin{aligned} &At\ \ \eta = 0 \Rightarrow f(\eta) = S,\ \ f'(\eta) = 1,\ \ \theta(\eta) = 1 - S_t,\ \ \phi(\eta) = 1 \\ &As\ \ \eta \to \infty \Rightarrow f' \to 0,\ \ \theta \to 0,\ \ \phi \to 1 \end{aligned}\right\} \tag{14}$$

Using Newton's method and using the concept of finite differences, the Eqs. 10-13 are reduced to Eq. 15.

$$\left.\begin{aligned} &(\delta f_j - \delta f_{j-1}) - 0.5h_j(\delta p_j + \delta p_{j-1}) = (r_1)_j \\ &(\delta p_j - \delta p_{j-1}) - 0.5h_j(\delta q_j + \delta q_{j-1}) = (r_2)_j \\ &(\delta g_j - \delta g_{j-1}) - 0.5h_j(\delta t_j + \delta t_{j-1}) + = (r_3)_j \\ &(\delta s_j - \delta s_{j-1}) - 0.5h_j(\delta n_j + \delta n_{j-1}) + = (r_4)_j \\ &(a_1)_j\delta q_j + (a_2)_j\delta q_{j-1} + (a_3)_j\delta g_j + (a_4)_j\delta g_{j-1} + (a_5)_j\delta t_j + (a_6)_j\delta t_{j-1} + (a_7)_j\delta p_j + (a_8)_j\delta p_{j-1} + (a_9)_j\delta f_j + (a_10)_j = (r_5)_j \\ &(b_1)_j\delta t_j + (b_2)_j\delta t_{j-1} + (b_3)_j\delta g_j + (b_4)_j\delta g_{j-1} + (b_5)_j\delta f_j + (b_6)_j\delta f_{j-1} + (b_7)_j\delta p_j + (b_8)_j\delta p_{j-1} = (r_6)_j \\ &(c_1)_j\delta n_j + (c_2)_j\delta n_{j-1} + (c_3)_j\delta f_j + (c_4)_j\delta f_{j-1} + (c_5)_j\delta s_j + (c_6)_j\delta s_{j-1} = (r_7)_j \end{aligned}\right\} \tag{15}$$

Where the $a's$ constant are determined from Eq. 16.

$$\left.\begin{aligned} (a_1)_j &= -\frac{(g_j+g_{j-1})\zeta}{2} - \frac{\zeta(t_j+t_{j-1})h_j}{4} + \frac{\beta(f_j+f_{j-1})h_j}{4(\beta+1)} + (1+\zeta-\zeta S_t) \\ (a_2)_j &= \frac{(g_j+g_{j-1})\zeta}{2} - \frac{\zeta(t_j+t_{j-1})h_j}{4} + \frac{\beta(f_j+f_{j-1})h_j}{4(\beta+1)} - (1+\zeta-\zeta S_t) \\ (a_3)_j = (a_4)_j &= -\frac{\zeta}{2}(q_j-q_{j-1}) - \frac{k\zeta h_j}{4}(p_j+p_{j-1}) + \frac{G_{rm}\beta\zeta h_j}{2(\beta+1)} \\ (a_5)_j = (a_6)_j &= -(q_j-q_{j-1})\frac{\zeta h_j}{4} \\ (a_7)_j &= -\frac{k\zeta h_j}{4}(g_j+g_{j-1})\frac{-kh_j}{2}(1+\zeta-\zeta S_t) - \frac{M\beta h_j}{2(\beta+1)} - \frac{\beta h_j}{\beta+1}(p_j+p_{j-1}) \\ (a_8)_j &= \frac{-kh_j}{2}(1+\zeta-\zeta S_t) - \frac{k\zeta h_j}{4}(g_j+g_{j-1}) - \frac{\beta h_j}{\beta+1}(p_j+p_{j-1}) - \frac{M\beta h_j}{2(\beta+1)} \\ (a_9)_j = (a_{10})_j &= \frac{\beta h_j}{2(\beta+1)}(q_j+q_{j-1}) \end{aligned}\right\} \tag{16}$$

And the $b's$ constants are determined from Eq. 17.

$$\left.\begin{aligned} (b_1)_j &= \frac{\varepsilon}{2}\left(\frac{3N}{3N+4}\right)(g_j+g_{j-1}) + \frac{3PrNh_j}{4(3N+4)}(f_j+f_{j-1}) + \frac{3\varepsilon Nh_j}{2(3N+4)}(t_j+t_{j-1}) + 1 \\ (b_2)_j &= -\frac{\varepsilon}{2}\left(\frac{3N}{3N+4}\right)(g_j+g_{j-1}) + \frac{3PrNh_j}{4(3N+4)}(f_j+f_{j-1}) + \frac{3\varepsilon Nh_j}{2(3N+4)}(t_j+t_{j-1}) - 1 \\ (b_3)_j = (b_4)_j &= \frac{\varepsilon}{2}\left(\frac{3N}{3N+4}\right)(t_j+t_{j-1}) + \frac{3PrNh_j}{4(3N+4)}(p_j+p_{j-1}) \\ (b_5)_j = (b_6)_j &= \frac{3PrNh_j}{4(3N+4)}(t_j+t_{j-1}) \\ (b_7)_j = (b_8)_j &= \frac{-3PrNS_t h_j}{2(3N+4)} - \frac{3PrNh_j}{4(3N+4)}(g_j+g_{j-1}) + \frac{1.5PrJNh_j}{3N+4}(p_j+p_{j-1}) \end{aligned}\right\} \tag{17}$$

Also, the $c's$ constant can be found from Eq. 18.

$$\left.\begin{aligned}
(c_1)_j &= -\frac{Sch_j}{4}\left(f_j+f_{j-1}\right)+1\\
(c_2)_j &= -2+(c_1)_j\\
(c_3)_j &= (c_4)_j = \frac{-Sch_j}{4}\left(n_j+n_{j-1}\right)\\
(c_5)_j &= (c_6)_j = \frac{-Sc\Gamma h_j}{2}
\end{aligned}\right\} \tag{18}$$

Finally, the $r's$ parameters are listed in Eq. 19.

$$\left.\begin{aligned}
(r_1)_j &= \frac{f_{j-1}-f_j}{h_j}-\frac{1}{2}\left(p_j+p_{j-1}\right)\\
(r_2)_j &= \frac{p_{j-1}-p_j}{h_j}-\frac{1}{2}\left(q_j+q_{j-1}\right)\\
(r_3)_j &= \frac{g_{j-1}-g_j}{h_j}-\frac{1}{2}\left(t_j+t_{j-1}\right)\\
(r_4)_j &= \frac{s_{j-1}-s_j}{h_j}-\frac{1}{2}\left(n_j+n_{j-1}\right)\\
(r_5)_j &= \frac{\zeta}{2}(g_{j-1}+g_j)(q_j+q_{j-1})+\frac{\zeta h_j}{4}\left(t_j+t_{j-1}\right)\left(q_j+q_{j-1}\right)+\frac{kh_j}{2}\left(1+\zeta-\zeta S_t\right)\left(p_j-p_{j-1}\right)+\frac{k\zeta h_j}{4}(g_{j-1}+g_j)(p_j+p_{j-1})+\\
&\quad +\left(1+\zeta-\zeta S_t\right)\left(q_{j-1}-q_j\right)-\frac{\beta h_j}{4(\beta+1)}\left(f_j+f_{j-1}\right)\left(q_j+q_{j-1}\right)\\
(r_6)_j &= t_{j-1}-\frac{\varepsilon\left(g_j+g_{j-1}\right)}{2}\left(\frac{3N}{3N+4}\right)\left(t_{j-1}-t_j\right)-\frac{3\varepsilon Nh_j}{3N+4}\left(t_j+t_{j-1}\right)^2-\frac{3PrNh_j}{4(3N+4)}\left(f_j+f_{j-1}\right)\left(t_j+t_{j-1}\right)+\frac{3PrNS_t h_j}{2(3N+4)}\left(p_j+p_{j-1}\right)+\\
&\quad +\frac{3PrNh_j}{4(3N+4)}\left(g_j+g_{j-1}\right)\left(p_j+p_{j-1}\right)-\frac{3PrNh_j q_1 e^{-n\eta}}{3N+4}-\frac{3PrNJh_j}{4(3N+4)}\left(p_j+p_{j-1}\right)^2-t_j\\
(r_7)_j &= n_{j-1}-n_j+\frac{Sch_j}{4}\left(f_j+f_{j-1}\right)\left(n_{j-1}+n_j\right)+\frac{Sc\Gamma h_j}{2}\left(s_j+s_{j-1}\right)
\end{aligned}\right\} \tag{19}$$

A tri-diagonal system Eq. 20- 23 are a representation of the equation system being used.

$$(A_1)=\begin{pmatrix}
0 & 0 & 0 & 1 & 0 & 0 & 0\\
-\frac{h_j}{2} & 0 & 0 & 0 & -\frac{h_j}{2} & 0 & 0\\
0 & -\frac{h_j}{2} & 0 & 0 & 0 & -\frac{h_j}{2} & 0\\
0 & 0 & -1 & 0 & 0 & 0 & -\frac{h_j}{2}\\
(a_2)_1 & (a_6)_1 & 0 & (a_9)_1 & (a_1)_1 & (a_5)_1 & 0\\
0 & (b_2)_1 & 0 & (b_5)_1 & 0 & (b_1)_1 & 0\\
0 & 0 & (c_6)_1 & (c_3)_1 & 0 & 0 & (c_1)_1
\end{pmatrix} \tag{20}$$

$$(A_j)=\begin{pmatrix}
-\frac{h_j}{2} & 0 & 0 & 1 & 0 & 0 & 0\\
-1 & 0 & 0 & 0 & -\frac{h_j}{2} & 0 & 0\\
0 & -1 & 0 & 0 & 0 & -\frac{h_j}{2} & 0\\
0 & 0 & -1 & 0 & 0 & 0 & -\frac{h_j}{2}\\
(a_8)_j & (a_4)_j & 0 & (a_9)_j & (a_1)_j & (a_5)_j & 0\\
(b_8)_j & (b_4)_j & 0 & (b_5)_j & 0 & (b_1)_j & 0\\
0 & 0 & (c_6)_j & (c_3)_j & 0 & 0 & (c_1)_j
\end{pmatrix} \tag{21}$$

$$(B_j)=\begin{pmatrix}
0 & 0 & 0 & -1 & 0 & 0 & 0\\
0 & 0 & 0 & 0 & -\frac{h_j}{2} & 0 & 0\\
0 & 0 & 0 & 0 & 0 & -\frac{h_j}{2} & 0\\
0 & 0 & 0 & 0 & 0 & 0 & -\frac{h_j}{2}\\
0 & 0 & 0 & (a_{10})_j & (a_2)_j & (a_6)_j & 0\\
0 & 0 & 0 & (b_6)_j & 0 & (b_2)_j & 0\\
0 & 0 & 0 & (c_4)_j & 0 & 0 & (c_2)_j
\end{pmatrix} \tag{22}$$

$$(C_j)=\begin{pmatrix}
-\frac{h_j}{2} & 0 & 0 & -1 & 0 & 0 & 0\\
1 & 0 & 0 & 0 & 0 & 0 & 0\\
0 & 1 & 0 & 0 & 0 & 0 & 0\\
0 & 0 & 1 & 0 & 0 & 0 & 0\\
(a_7)_j & (a_3)_j & 0 & 0 & 0 & 0 & 0\\
(b_7)_j & (b_3)_j & 0 & 0 & 0 & 0 & 0\\
0 & 0 & (c_5)_j & 0 & 0 & 0 & 0
\end{pmatrix} \tag{23}$$

3. Results and discussion

MATLAB is used to plot the graphs in order to conduct an analysis of the situation. The results are in agreement with the existing literature, which is displayed in Table 1. The numerical validation of the data is accomplished by comparing them with previous literature and computing the Nusselt number for expanding observations of the Prandtl number.

Table 1. A comparative study with the previous studies.

Pr	Animasun et al. [36]	Agrawal et al. [35]	Present study
1	0.679607	0.679607	0.685270
2	1.073523	1.073523	1.051267
3	1.380709	1.380709	1.383749

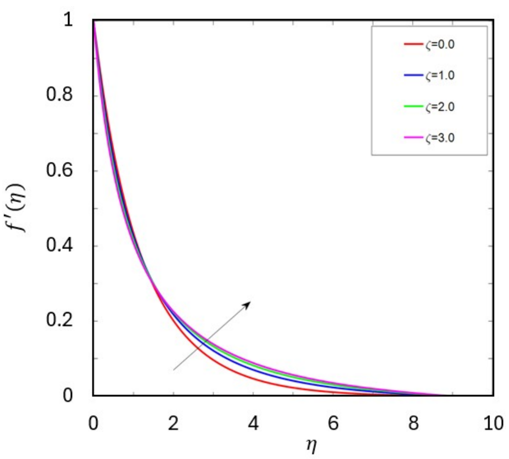

Figure 2. Velocity outlines of viscosity constraint.

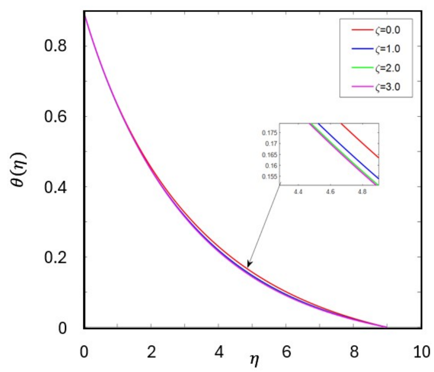

Figure 3. Temperature outlines of Viscosity constraint.

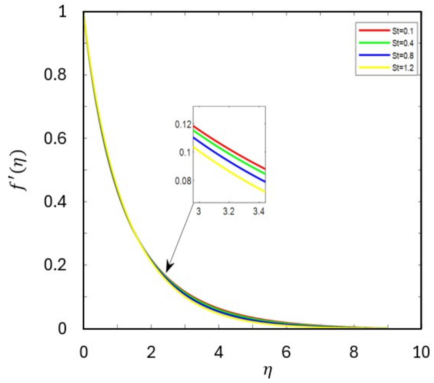

Figure 4. Velocity outlines of stratification constraint.

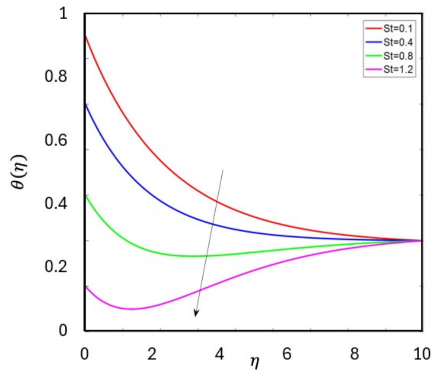

Figure 5. Temperature graphs of the stratification parameter.

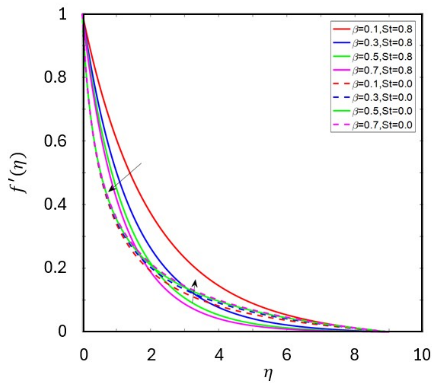

Figure 6. Velocity graphs of Casson parameter.

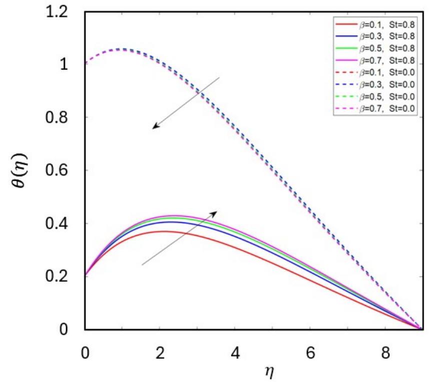

Figure 7. Temperature graphs of the Casson parameter.

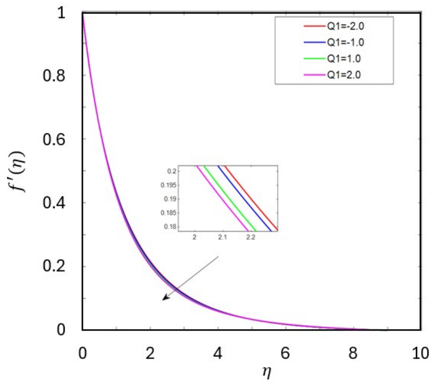

Figure 8. Velocity outlines for the heat source parameter.

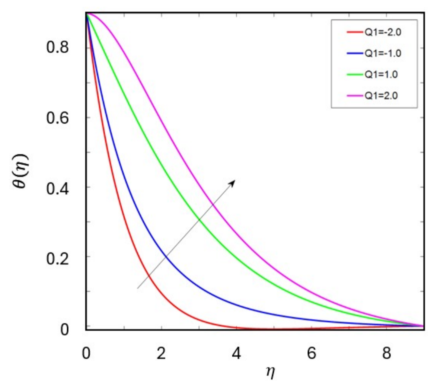

Figure 9. Temperature graphs of heat source argument.

The interaction between the viscous force and the shear rate determines viscosity. A Casson fluid's velocity profile increases while staying constant when its plastic dynamic viscosity rises. Moreover, as seen in Fig. 2 and Fig. 3, a drop in the temperature profile is noted. Temperature profiles and stratification parameter velocity are observed to be growing, as the temperature increase in the vicinity of the surface is more than in the border region. Figure 4 and Fig. 5 illustrate that. The boundary layer thickness reduces with increasing Casson constraint momentum data. It is found that profiles of velocity decrease. Increasing the Casson argument's thermal marginal layer width results in higher temperature profiles. In the absence of a stratification parameter, a change in thermal conductivity is directly correlated with an increase in the temperature profile. When stratification is present, as Fig. 6 and Fig. 7 show, the impact is reversed. Figure 8 and Fig. 9 illustrate the relationship between the heat generation parameter and velocity, where a rise in the parameter results in a drop in velocity and an increase in temperature.

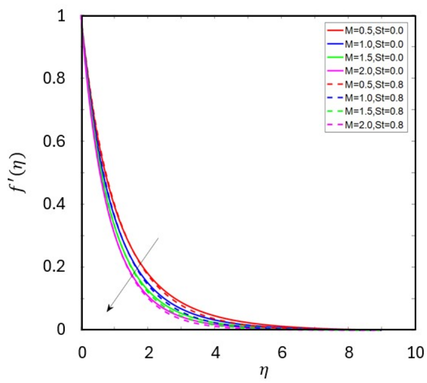

Figure 10**.** Velocity graphs of Magnetic constraint.

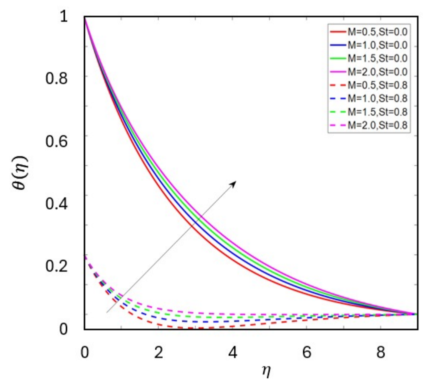

Figure 11**.** Temperature graphs of Magnetic constraint.

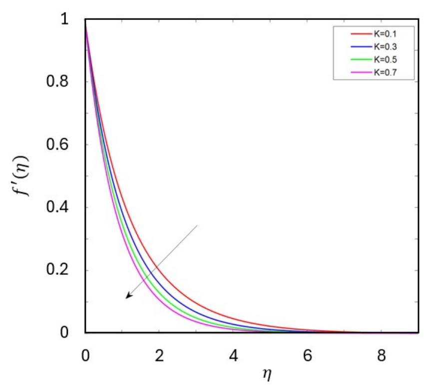

Figure 12**.** Velocity graphs of porosity parameter.

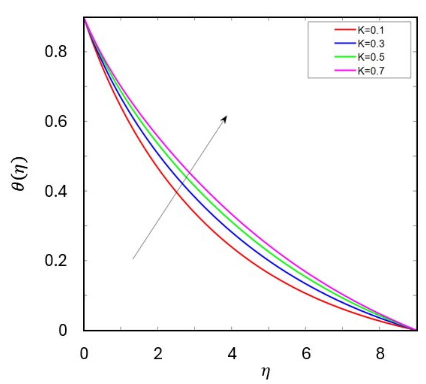

Figure 13**.** Temperature outlines of porosity parameter.

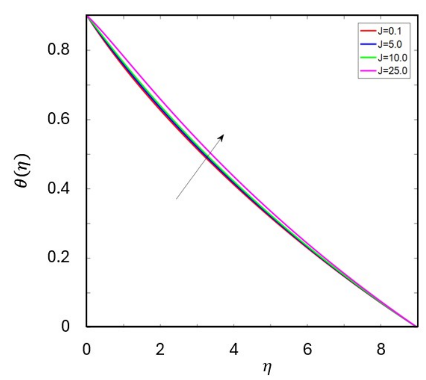

Figure 14**.** Temperature outlines of Joule heating parameter.

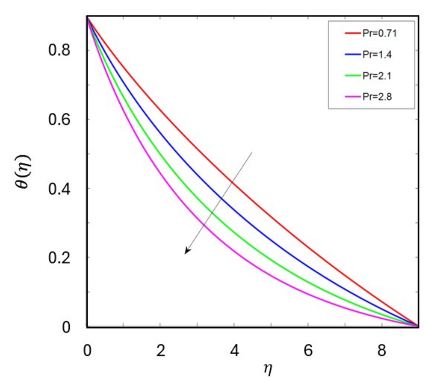

Figure 15**.** Temperature graphs of Prandtl number.

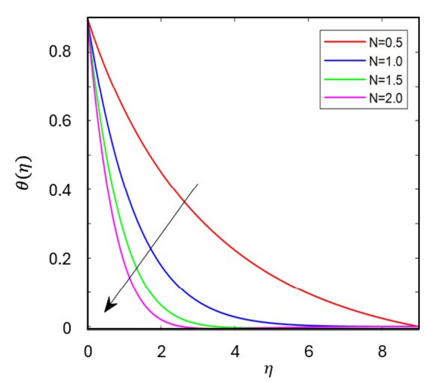

Figure 16**.** Temperature graphs of radiation constraint.

The Lorentz force is produced when the magnetic parameter increases. The velocity profiles fall as a result of this force's opposing action. Furthermore, the temperature profiles are rising, as shown in Fig. 10 and Fig. 11. As porosity parameter profiles grow, temperature increases, and velocity falls. Figure 12 and Fig. 13 illustrate how a fluid's velocity decreases as porosity increases because a porous medium's permeability increases. The procedure for converting electrical energy into heat energy by raising the joule heating parameter is shown in Fig. 14. The fluid's decreasing thermal conductivity as the Prandtl number rises is seen in Fig. 15, which results in a drop in temperature. The temperature drop that occurs when the radiation parameter is increased is shown in Fig. 16. This is due to the fact that radiation lowers the fluid's rate of energy transmission. When Grashoff argument is strengthened, the temperature decreases. As the grashoff number rises, buoyancy force develops and, as a result, the thickness of the thermal boundary layer in Fig. 17 decreases. The Schmidt number concentration profiles are shown in Fig. 18. The concentration profile is demonstrated to decrease as mass transfer increases because the Schmidt number rises.

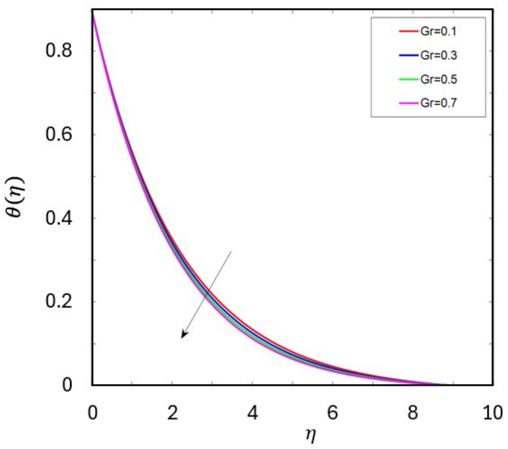

Figure 17**.** Temperature outlines of Grashoff number.

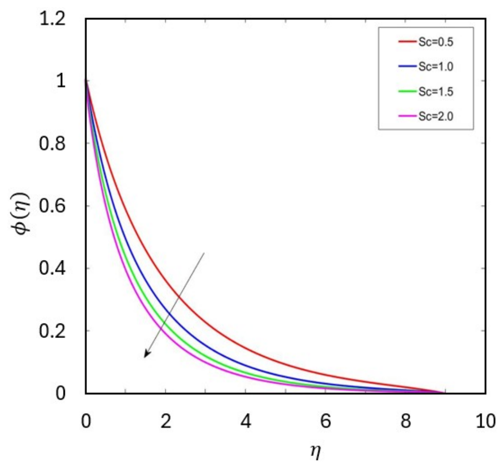

Figure 18**.** Concentration outlines of Schmidt number.

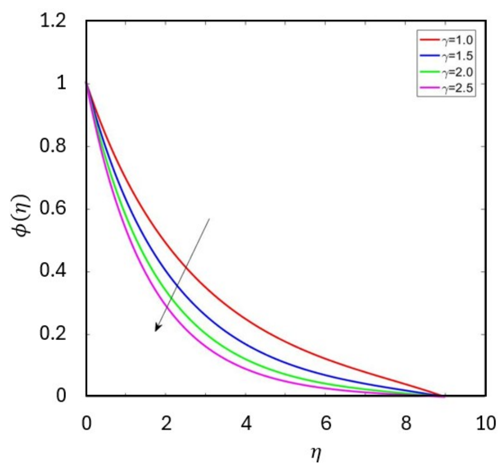

Figure 19**.** Concentration outlines of the Chemical reaction parameter.

The diffusivity of the chemical molecules decreases with increasing values of the chemical reaction argument, which results in a decrease in the reported concentration profiles. Figure 19 portrays that the Diffusivity of chemical molecules diminishes as the values of reactiveness increase, leading to reduction in observed concentration profiles. The thermal conductivity increases with increase in temperature due to higher temperature causing molecules to vibrate more vigorously shown in Fig. 20.

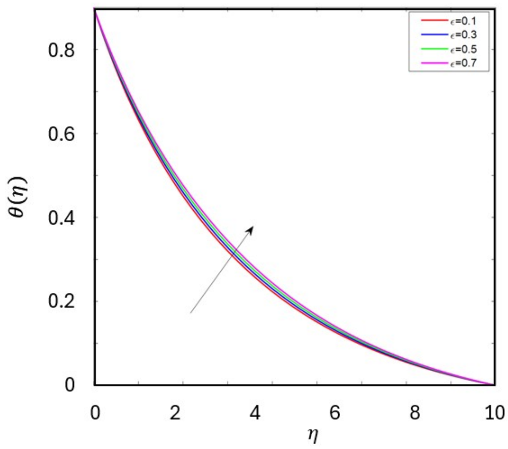

Figure 20**.** Temperature outlines of the Thermal conductivity parameter.

4. Conclusions

Here, we explore a two-dimensional Casson flow across an exponentially stretched sheet in thermally stratified porous media. We solve the fluid flow equations by applying the Keller Box method. The features of mass and heat transport can be examined by making profile graphs of concentration, temperature, and velocity. The Nusselt number is calculated and compared with relevant literature as part of the numerical approach validation phase. It appears that the outcomes support the findings of the earlier investigation. Because the study is significant to MHD, Joule heating, chemical reactions, non-Newtonian fluids, and heat source attributes, we talked about it. There are several reasons why the velocity profile might increase. The stratification parameter, the porosity parameter, the magnetic parameter, the progressive observations of plastic dynamic viscosity, and the stratification parameter decrease without a stratification parameter, and Casson arguments with a stratification parameter are some of these variables. The temperature profile drops in the presence of plastic dynamic viscosity and stratification effects. In the absence of stratification, the temperature profile rises for every given Casson value. The magnetic parameter, the heat source, the porosity, and the Joule heating parameters show signs of an increase in both situations. It appears that nothing has changed with regard to the radiation argument, the thermal Grashof number, and the Prandtl number. The concentration profile appears to be more flattened when considering the Schmidt number and the chemical reaction parameter. Additionally, the Nusselt number is increased to enhance the Prandtl coefficient.

Authors' contribution

All authors contributed equally to the preparation of this article.

Declaration of competing interest

The authors declare no conflicts of interest.

Funding source

This study didn't receive any specific funds.

Data availability

The data that support the findings of this study are available from the corresponding author upon reasonable request.

REFERENCES

[1] A. V. Shenoy, "Non-newtonian fluid heat transfer in porous media," *Advances in Heat transfer*, vol. 24, pp. 101–190, 1994. [Online]. Available: https://doi.org/10.1016/S0065-2717(08)70233-8

[2] A. J. Chamkha and J. M. Al-Humoud, "Mixed convection heat and mass transfer of non-newtonian fluids from a permeable surface embedded in a porous medium," *International Journal of Numerical Methods for Heat Fluid Flow,*, vol. 17, no. 2, pp. 195–212, 2007. [Online]. Available: https://doi.org/10.1108/09615530710723966

[3] R. Kairi and P. Murthy, "Effect of viscous dissipation on natural convection heat and mass transfer from vertical cone in a non-newtonian fluid saturated non-darcy porous medium," *Applied Mathematics and Computation*, vol. 217, no. 20, p. 8100–8114, 2011. [Online]. Available: http://dx.doi.org/10.1016/j.amc.2011.03.013

[4] R. Gorla, S. Asghar, M. Hossain, W. Khan, and S. Mukhopadhyay, "Heat and mass transfer in non-newtonian fluids," *Advances in Mechanical Engineering*, vol. 6, p. 104392, 2014. [Online]. Available: https://doi.org/10.1155/2014/104392

[5] A. Sinha and G. C. Shit, "Role of slip velocity on the oscillatory flow of blood through a porous vessel in the presence of heat source and chemical reaction," *Journal of Mechanics*, vol. 30, no. 2, pp. 209–218, 2014. [Online]. Available: https://doi.org/10.1017/jmech.2014.15

[6] N. El-Dabe, A. Ghaly, R. Rizkallah, K. Ewis, and A. Al-Bareda, "Numerical solution of mhd boundary layer flow of non-newtonian casson fluid on a moving wedge with heat and mass transfer and induced magnetic field," *Journal of Applied Mathematics and Physics*, vol. 3, no. 6, pp. 649–663, 2015. [Online]. Available: https://doi.org/10.4236/jamp.2015.36078

[7] N. Singh and R. Yadav, "Investigation of heat transfer of non-newtonian fluid in the presence of a porous wall," *International Journal of Engineering Technologies and Management Research*, vol. 4, no. 12, pp. 74–92, 2017. [Online]. Available: https://doi.org/10.29121/ijetmr.v4.i12.2017.137

[8] K. Vajravelu, K. Prasad, H. Vaidya, N. Basha, and O. Ng, "Mixed convective flow of a casson fluid over a vertical," . *Math. Comp*, vol. 184, pp. 864–873, 2007. [Online]. Available: https://doi.org/10.1007/s40819-016-0203-6

[9] H. Attia and M. E. Sayed-Ahmed, "Transient mhd couette flow of a casson fluid between parallel plates with heat transfer," *Italian Journal of pure and applied Mathematics*, vol. 27, 2010.

[10] S. Shehzad, T. Hayat, M. Qasim, and S. Asghar, "Effects of mass transfer on mhd flow of casson fluid with chemical reaction and suction," *Brazilian Journal of Chemical Engineering*, vol. 30, no. 1, pp. 187–195, 2013. [Online]. Available: https://doi.org/10.1590/S0104-66322013000100020

[11] B. Gireesha, B. Mahanthesh, and M. M. Rashidi, "Mhd boundary layer heat and mass transfer of a chemically reacting casson fluid over a permeable stretching surface with non-uniform heat source/sink," *Int. J. Industrial Mathematics*, vol. 7, no. 3, pp. 247–260, 2015. [Online]. Available: Availableonlineathttp://ijim.srbiau.ac.ir/

[12] I. L. Animasaun, "Effects of thermophoresis, variable viscosity and thermal conductivity on free convective heat and mass transfer of non-darcian mhd dissipative casson fluid flow with suction and nth order of chemical reaction," *Journal of the Nigerian Mathematical Society*, vol. 34, no. 1, pp. 11–31, 2015. [Online]. Available: https://doi.org/10.1016/j.jnnms.2014.10.008

[13] A. Hussanan, M. Z. Salleh, H. Alkasasbeh, and I. Khan, "Mhd flow and heat transfer in a casson fluid over a nonlinearly stretching sheet with newtonian heating," *Heat transfer research*, vol. 49, no. 12, pp. 1185–1198, 2018. [Online]. Available: https://doi.org/10.1615/HeatTransRes.2018014771âĂŔ

[14] S. Ibrahim, P. Kumar, and G. Lorenzini, "Analytical modeling of heat and mass transfer of radiative mhd casson fluid over an exponentially permeable stretching sheet with chemical reaction," *Journal of Engineering Thermophysics*, vol. 29, no. 1, pp. 136–155, 2020. [Online]. Available: https://doi.org/10.1134/S1810232820010105

[15] G. Ganesh and W. Sridhar, "Mhd radiative casson—nanofluid stream above a nonlinear extending surface including chemical reaction through darcy-forchiemer medium," *Heat Transfer Portico.*, vol. 50, no. 8, p. 7691–7711, July 2021. [Online]. Available: https://doi.org/10.1002/htj.22249

[16] W. Sridhar, T. Hymavathi, S. E. Ahmed, A. Alenazi, and G. Ganesh, "Keller box procedure for stagnation point flow of emhd casson nanofluid over an absorbent stretched electromagnetic plate with chemical reaction," *Numerical Heat Transfer, Part A: Applications*, vol. 85, no. 17, p. 1–18, 2024. [Online]. Available: https://doi.org/10.1080/10407782.2023.2229949

[17] K. Al-Farhany and M. Al-Maliki, "Experimental investigation of heat transfer in a cavity filled with (50% cuo-50% al2o3)/water with hybrid nanofluid attached to a vertically heated wall partially integrated with pcm," *Al-Qadisiyah Journal for Engineering Sciences*, vol. 16, no. 1, p. 21–29, 2023. [Online]. Available: https://doi.org/10.30772/qjes.v16i1.912

[18] M. A. G. and K. B. Kh. Al-Farhany, "Effects of fin on mixed convection heat transfer in a vented square cavity: A numerical study," *Al-Qadisiyah Journal for Engineering Sciences*, vol. 16, no. 3, p. 200–208, 2023. [Online]. Available: https://doi.org/10.30772/qjes.2023.142305.1016

[19] A. Kamran, S. Hussain, M. Sagheer, and N. Akmal, "A numerical study of magneto- hydrodynamics flow in casson nanofluid combined with joule heating and slip boundary conditions," *Results in physics*, vol. 7, no. 2017, pp. 3037–3048, 2017. [Online]. Available: https://doi.org/10.1016/j.rinp.2017.08.004

[20] E. Khoshrouye Ghiasi and R. Saleh, "2d flow of casson fluid with non-uniform heat source/sink and joule heating," *Frontiers in Heat and Mass Transfer*, vol. 12, no. 1, pp. 1–7, January 2019. [Online]. Available: https://doi.org/10.5098/hmt.12.4

[21] B. S. Goud, Y. D. Reddy, V. S. Rao, and Z. H. Khan, "Thermal radiation and joule heating effects on a magnetohydrodynamic casson nanofluid flow in the presence of chemical reaction through a non-linear inclined porous stretching sheet." *Journal of Naval Architecture Marine Engineering*, vol. 17, no. 2, pp. 143–164, 2020. [Online]. Available: http://doi.org/10.3329/jname.v17i2.49978

[22] S. Jaffrullah, W. Sridhar, and G. R. Ganesh, "Mhd radiative casson fluid flow through forchheimer permeable medium with joule heating influence," *CFD Letters*, vol. 15, no. 8, p. 179–199, September 2023. [Online]. Available: https://doi.org/10.37934/cfdl.15.8.179199

[23] O. D. Makinde, "Mhd mixed-convection interaction with thermal radiation and nth order chemical reaction past a vertical porous plate embedded in a porous medium," *Chemical Engineering Communications*, vol. 198, no. 4, pp. 590–608, 2010. [Online]. Available: http://doi.org/10.1080/00986445.2010.500151

[24] H. M. Shawky, "Magnetohydrodynamic casson fluid flow with heat and mass transfer through a porous medium over a stretching sheet," *Journal of Porous Media*, vol. 15, no. 4, pp. 393–401, 2012. [Online]. Available: https://doi.org/10.1615/JPorMedia.v15.i4.70

[25] F. Mabood, W. Khan, and A. Ismail, "Multiple slips effects on mhd casson fluid flow in porous media with radiation and chemical reaction," *Canadian Journal of Physics*, vol. 94, no. 1, pp. 26–34, 2016. [Online]. Available: https://doi.org/10.1139/cjp-2014-0667

[26] U. M. B. Al-Naib, "investigation of heat transfer characteristics of al2o3-water nanofluid in a coiled agitated vessel across varied operating conditions," *Al-Qadisiyah Journal for Engineering Sciences*, vol. 16, no. 3, p. 145–149, 2023. [Online]. Available: https://doi.org/10.30772/qjes.2023.178993

[27] G. R. Ganesh and W. Sridhar, "Effect of chemical reaction towards mhd marginal layer movement of casson nanofluid through porous media above a moving plate with an adaptable thickness," *Pertanika Journal of Science and Technology*, vol. 30, no. 1, p. 477–495, 2022. [Online]. Available: https://doi.org/10.47836/pjst.30.1.26

[28] R. Mahesh, U. Mahabaleshwar, E. H. Aly, and O. Manca, "An impact of cnts on an mhd casson marangoni boundary layer flow over a porous medium with suction/injection and thermal radiation," *International Communications in Heat and Mass Transfer*, vol. 141, p. 106561, 2023. [Online]. Available: https://doi.org/10.1016/j.icheatmasstransfer.2022.106561

[29] T. Yusuf, R. Kareem, S. Adesanya, and J. Gbadeyan, "Entropy generation on mhd flow of a casson fluid over a curved stretching surface with exponential space-dependent heat source and nonlinear thermal radiation," *Heat Transfer*, vol. 51, no. 2, pp. 2079–2098, 2021. [Online]. Available: https://doi.org/10.1002/htj.22389

[30] P. Pattnaik, S. Mishra, B. Mahanthesh, B. Gireesha, and M. Rahimi-Gorji, "Heat transport of nano-micropolar fluid with an exponential heat source on a convectively heated elongated plate using numerical computation," *Multidiscipline Modeling in Materials and Structures*, vol. 16, no. 5, pp. 1295–1312, 2020. [Online]. Available: https://doi.org/10.1108/MMMS-12-2018-0222

[31] H. Waqas, U. Farooq, A. Ibrahim, M. Kamran Alam, Z. Shah, and P. Kumam, "Numerical simulation for bioconvectional flow of burger nanofluid with effects of activation energy and exponential heat source/sink over an inclined wall under the swimming microorganisms," *Scientific Reports*, vol. 11, no. 1, p. 14305, 2021. [Online]. Available: https://doi.org/10.1038/s41598-021-93748-x

[32] A. Kumar, B. Sharma, R. Gandhi, N. Mishra, and M. M. Bhatti, "Response surface optimization for the electromagnetohydrodynamic cu-polyvinyl alcohol/water jeffrey nanofluid flow with an exponential heat source," *Journal of Magnetism and Magnetic Materials*, vol. 576, p. 170751, 2023. [Online]. Available: https://doi.org/10.1016/j.jmmm.2023.170751

[33] A. Amendola, T. Ermolieva, J. Linnerooth-Bayer, and R. Mechler, “Flow and transport in porous formations,” *Springer Science Business Media*, 2012. [Online]. Available: https://doi.org/10.1007/978-94-007-2226-2

[34] H. T. Malik, M. Farooq, S. Ahmad, and M. M. Mohamed, “Convective heat transportation in exponentially stratified casson fluid flow over an inclined sheet with viscous dissipation,” *Case Studies in Thermal Engineering*, vol. 52, no. 2023, p. 103720, 2023. [Online]. Available: 52,.https://doi.org/10.1016/j.csite.2023.103720âĂŘ

[35] P. Agrawala, P. Dadheech, R. Jat, D. Baleanu, and S. Purohit, “Exploration of casson fluid-flow along exponential heat source in a thermally stratified porous media,” *Thermal Science J.*, vol. 27, no. 1, p. 29–38, 2023. [Online]. Available: https://doi.org/10.2298/tsci23s1029a

[36] I. L. Animasaun, “Casson fluid-flow with variable viscosity and thermal conductivity along exponentially stretching sheet embedded in a thermally stratified medium with exponentially heat generation,” *Journal of Heat and Mass Transfer Research*, vol. 2, no. 2, pp. 63–78, 2015. [Online]. Available: https://doi.org/10.22075/jhmtr.2015.346

How to cite this article:
G. Raghavendra Ganesh, Shaik Jaffrullah, Wuriti Sridhar, Khaled Al-Farhany, Mohamed F. Al-Dawody, and Mujtaba A. Flayyih. (2025). ’Influence of joule heating and exponential heat source on the cassonfluid flow through a thermally graded permeable medium’, Al-Qadisiyah Journal for Engineering Sciences, 18(3), pp. 298- 306. `https://doi.org/10.30772/qjes.2025.163822.1687`